Local and non-local features in the primordial power spectrum and associated non-Gaussianities

Dhiraj Kumar Hazra

Harish-Chandra Research Institute, Allahabad, India

Institut d'Astrophysique de Paris (IAP), Paris, France

Introduction: Primordial features and non-Gaussianities

Outliers in the WMAP data can indicate features in the primordial power spectrum and features can lead to a better fit to the CMB data when compared with the featureless slow roll inflationary power spectrum

Introduction: Primordial features and non-Gaussianities

Outliers in the WMAP data can indicate features in the primordial power spectrum and features can lead to a better fit to the CMB data when compared with the featureless slow roll inflationary power spectrum

... I shall discuss the origin and the effects of the features in the PPS

Introduction: Primordial features and non-Gaussianities

Outliers in the WMAP data can indicate features in the primordial power spectrum and features can lead to a better fit to the CMB data when compared with the featureless slow roll inflationary power spectrum

... I shall discuss the origin and the effects of the features in the PPS

Non-Gaussianities are turning to be a useful tool to characterize inflationary models,

Large non-Gaussianities can be achieved by deviation from,

- Slow roll inflation
- Canonical scalar field driven inflation
- Single field driven inflation
- Bunch-Davies vaccum initial condition

Introduction: Primordial features and non-Gaussianities

Outliers in the WMAP data can indicate features in the primordial power spectrum and features can lead to a better fit to the CMB data when compared with the featureless slow roll inflationary power spectrum

... I shall discuss the origin and the effects of the features in the PPS

Non-Gaussianities are turning to be a useful tool to characterize inflationary models,

Large non-Gaussianities can be achieved by deviation from,

- Slow roll inflation
- Canonical scalar field driven inflation
- Single field driven inflation
- Bunch-Davies vaccum initial condition

Outline of the talk

1. Localized oscillations in the primordial power spectrum with a step
    - Slow-roll inflation
    - How features in the PPS can fit the outliers
    - Effects of the step
    - The goal of our project
    - Results
    - Summary and discussion

Outline of the talk

1. Localized oscillations in the primordial power spectrum with a step
   - Slow-roll inflation
   - How features in the PPS can fit the outliers
   - Effects of the step
   - The goal of our project
   - Results
   - Summary and discussion

2. Non-local features
   - Possibilities of non-local features
   - Does the data support non-local features?
   - The goal of our project
   - Results
   - Summary and discussion

Outline of the talk

1. Localized oscillations in the primordial power spectrum with a step
   - Slow-roll inflation
   - How features in the PPS can fit the outliers
   - Effects of the step
   - The goal of our project
   - Results
   - Summary and discussion
2. Non-local features
   - Possibilities of non-local features
   - Does the data support non-local features?
   - The goal of our project
   - Results
   - Summary and discussion
3. Calculating non-Gaussianities
   - Essentials
   - Calculating non-Gaussianities for the Starobinsky model
   - Our Numerical analysis
   - Summary and discussion

Proliferation of inflationary models[1]

5-dimensional assisted inflation
anisotropic brane inflation
anomaly-induced inflation
assisted inflation
assisted chaotic inflation
boundary inflation
brane inflation
brane-assisted inflation
brane gas inflation
brane-antibrane inflation
braneworld inflation
Brans-Dicke chaotic inflation
Brans-Dicke inflation
bulky brane inflation
chaotic hybrid inflation
chaotic inflation
chaotic new inflation
D-brane inflation
D-term inflation
dilaton-driven inflation
dilaton-driven brane inflation
double inflation
double D-term inflation
dual inflation
dynamical inflation
dynamical SUSY inflation
eternal inflation
extended inflation
extended open inflation
extended warm inflation
extra dimensional inflation
F-term inflation
F-term hybrid inflation
false vacuum inflation
false vacuum chaotic inflation
fast-roll inflation
first order inflation
gauged inflation
generalised inflation
generalized assisted inflation
generalized slow-roll inflation
gravity driven inflation
Hagedorn inflation
higher-curvature inflation
hybrid inflation
hyperextended inflation
induced gravity inflation
induced gravity open inflation
intermediate inflation
inverted hybrid inflation
isocurvature inflation
K inflation
kinetic inflation
lambda inflation
large field inflation
late D-term inflation
late-time mild inflation
low-scale inflation
low-scale supergravity inflation
M-theory inflation
mass inflation
massive chaotic inflation
moduli inflation
multi-scalar inflation
multiple inflation
multiple-field slow-roll inflation
multiple-stage inflation
natural inflation
natural Chaotic inflation
natural double inflation
natural supergravity inflation
new inflation
next-to-minimal supersymmetric hybrid inflation
non-commutative inflation
non-slow-roll inflation
nonminimal chaotic inflation
old inflation
open hybrid inflation
open inflation
oscillating inflation
polynomial chaotic inflation
polynomial hybrid inflation
power-law inflation
pre-Big-Bang inflation
primary inflation
primordial inflation
quasi-open inflation
quintessential inflation
R-invariant topological inflation
rapid asymmetric inflation
running inflation
scalar-tensor gravity inflation
scalar-tensor stochastic inflation
Seiberg-Witten inflation
single-bubble open inflation
spinodal inflation
stable starobinsky-type inflation
steady-state eternal inflation
steep inflation
stochastic inflation
string-forming open inflation
successful D-term inflation
supergravity inflation
supernatural inflation
superstring inflation
supersymmetric hybrid inflation
supersymmetric inflation
supersymmetric topological inflatior
supersymmetric new inflation
synergistic warm inflation
TeV-scale hybrid inflation

A (partial?) list of ever-increasing number of inflationary models. May be, we should look for models that permit deviations from the standard picture of slow roll inflation.

[1] From E. P. S. Shellard, *The future of cosmology: Observational and computational prospects*, in *The Future of Theoretical Physics and Cosmology*, Eds. G. W. Gibbons, E. P. S. Shellard and S. J. Rankin (Cambridge University Press, Cambridge, England, 2003).

1 Localized oscillations in the primordial power spectrum with a step
- Slow-roll inflation
- How features in the PPS can fit the outliers
- Effects of the step
- The goal of our project
- Results
- Summary and discussion

2 Non-local features
- Possibilities of non-local features
- Does the data support non-local features?
- The goal of our project
- Results
- Summary and discussion

3 Calculating non-Gaussianities
- Essentials
- Calculating non-Gaussianities for the Starobinsky model
- Our Numerical analysis
- Summary and discussion

Based on work with M. Aich, R. K. Jain, L. Sriramkumar and T. Souradeep

Ref: JCAP 1010:008, 2010

Angular power spectrum from the WMAP 7-year data

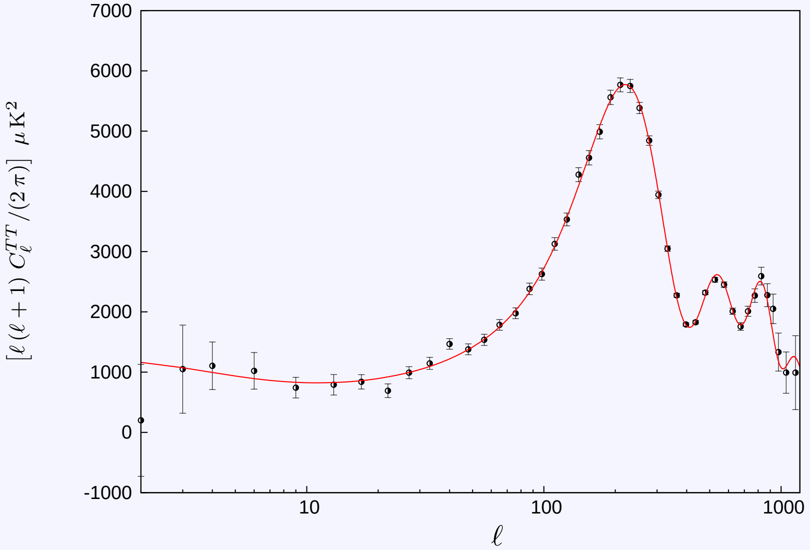

Angular power spectrum from the WMAP 7-year data

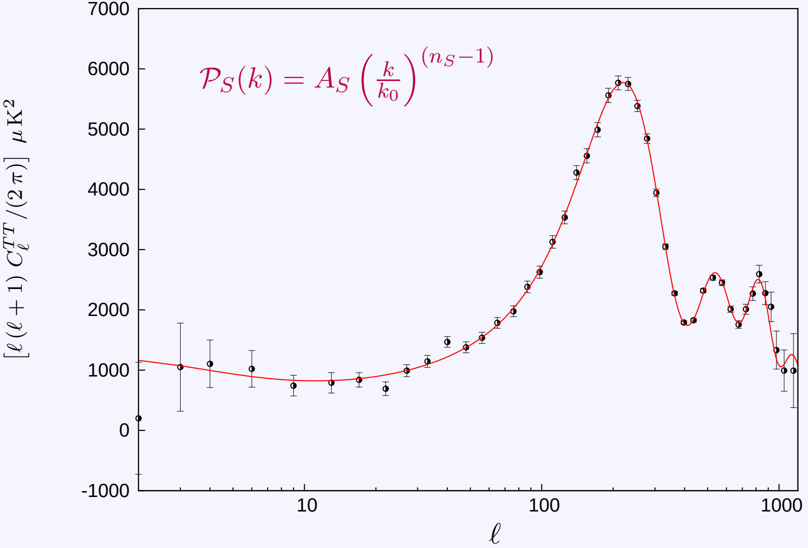

Angular power spectrum from the WMAP 7-year data

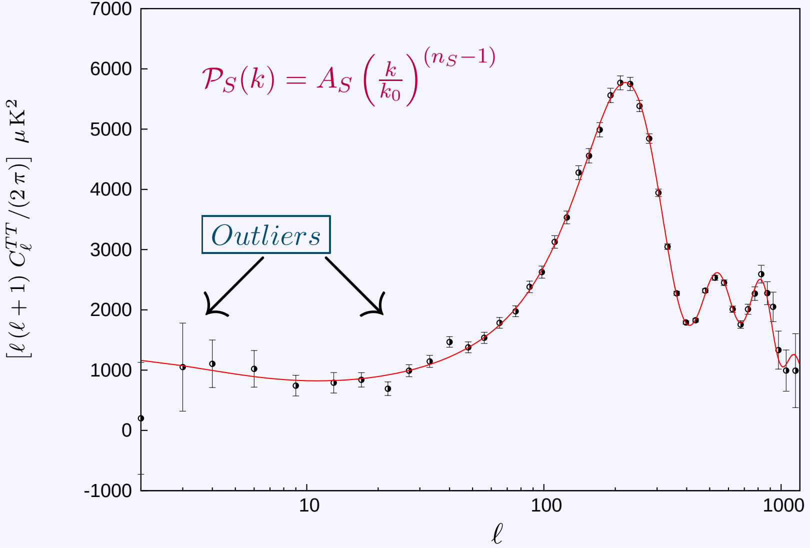

WMAP-7 year data: What outliers may indicate

Features

- Theoretical primordial power spectrum predicted by conventional slow roll inflation matches the CMB data very well
- There exists some outliers in the data that may indicate features in the primordial power spectrum
- It has been shown in earlier literature that certain features in the PPS can lead to an improvement in fit when compared with the standard featureless PPS generated by slow roll inflation
- Features might indicate certain non-trivial inflationary dynamics

Indication

This may lead to certain deviation from the conventional slow roll inflation

The scalar power spectrum in slow roll inflation

- The power law scalar power spectrum, and the spectrum from the quadratic potential $(m^2\phi^2/2)$ are shown below. They are almost indistinguishable, and they fit the data to the same extent.

Blue $=$ $m^2\phi^2/2$ case
Red $=$ The powerlaw primordial power spectrum

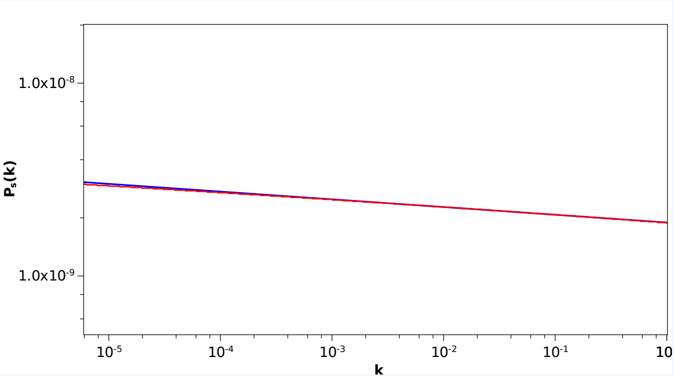

Angular power spectrum in slow roll inflation

- Standard slow roll inflation produces almost the same angular power spectrum as a power law primordial spectrum
- We have plotted below the CMB angular power spectrum for the best fit values of the canonical scalar field described by the quadratic potential.

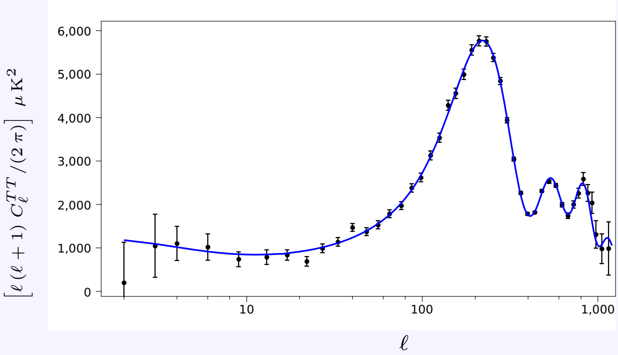

Localized features in the PPS

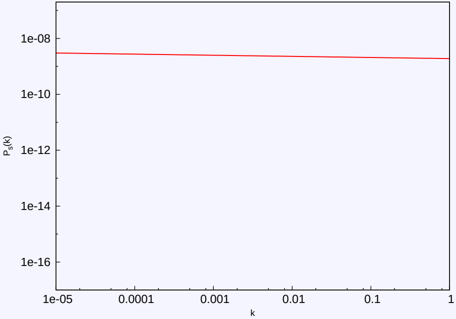

- Certain oscillatory features in the primordial scalar power spectrum are known to provide a better fit to the data

Localized features in the PPS

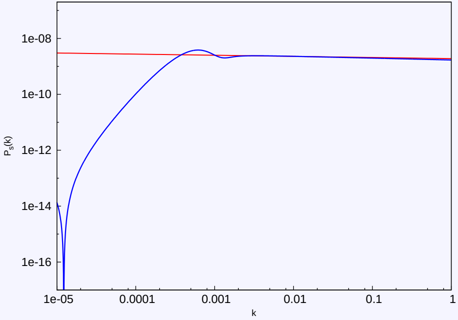

- Certain oscillatory features in the primordial scalar power spectrum are known to provide a better fit to the data
- For example, punctuated inflation[a] is known to lead to a better fit to the outliers near $\ell = 2$ and $\ell = 22$ than the standard power law spectrum

[a] Jain et. al.(2009)

Potential for the PI

$$V(\phi) = \left(\frac{m^2}{2}\right)\,\phi^2 - \left(\frac{2\sqrt{\lambda}\,m}{3}\right)\,\phi^3 + \left(\frac{\lambda}{4}\right)\,\phi^4,$$

Localized features in the PPS

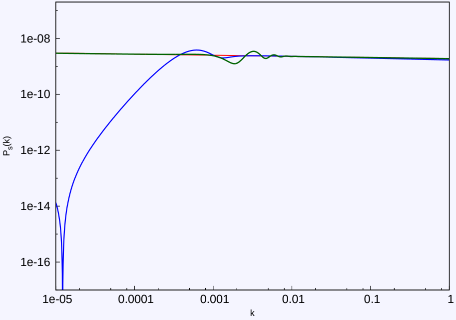

- Certain oscillatory features in the primordial scalar power spectrum are known to provide a better fit to the data
- For example, punctuated inflation[a] is known to lead to a better fit to the outliers near $\ell = 2$ and $\ell = 22$ than the standard power law spectrum
- The oscillatory features can also be generated with the introduction of a step[b] in a potential which provides better fit to the CMB data near $\ell = 22$ and $\ell = 40$

[a] Jain et. al.(2009)

[b] Adams et. al.(2001); Covi et. al.(2006); Mortonson et. al.(2009); Hazra et. al.(2010)

Potential for the PI — Potential for the step

$$V(\phi) = \left(\frac{m^2}{2}\right)\phi^2 - \left(\frac{2\sqrt{\lambda}\, m}{3}\right)\phi^3 + \left(\frac{\lambda}{4}\right)\phi^4, \tilde{V}(\phi) = V(\phi) \times \left[1 + \alpha \tanh\left(\frac{\phi - \phi_0}{\Delta\phi}\right)\right]$$

Localized features in the PPS

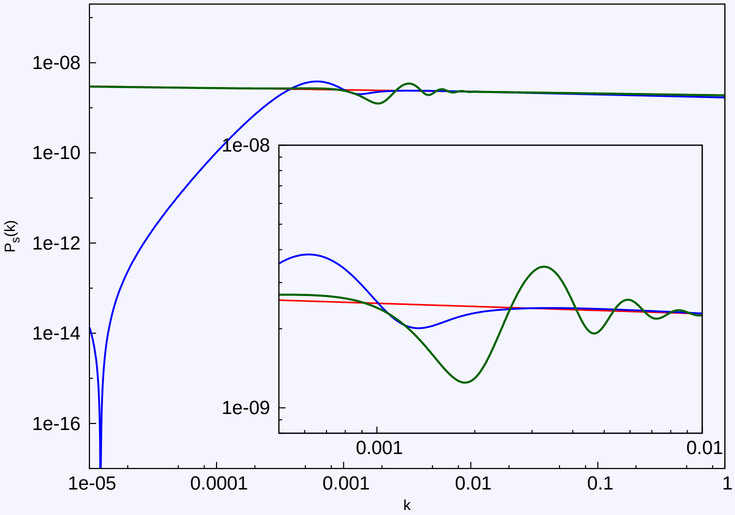

The slow roll parameters

- The following two parameters characterize slow roll inflation

The Hubble slow-roll parameters

$$\epsilon = -\frac{\dot{H}}{H^2}, \qquad \eta = -\frac{\ddot{\phi}}{H\dot{\phi}}$$

If the inflaton is rolling slowly down a potential, then $(\epsilon,\ \eta) << 1$

- When we introduce a step in the potential, the field experiences a fast roll near the location of the step (ϕ_0)
- The parameter α determines the strength of the step and $\Delta\phi$ characterizes its width
- These parameters can be used to can tune the location, the strength and the duration of the fast roll period

Behavior of ϵ and η during fast roll

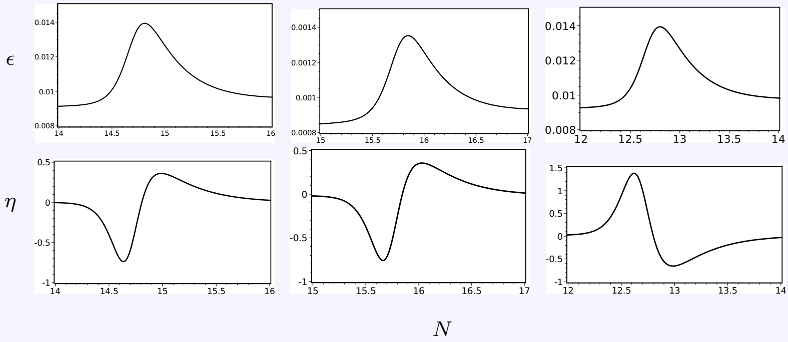

Quadratic model Small field model Tachyon model

The behavior of the first two slow roll parameters for a few different models as the field crosses the step

Effects of α

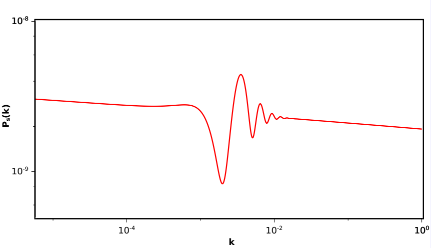

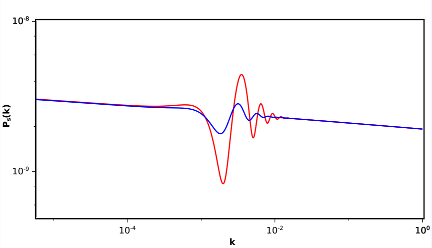

Effects of ϕ_0

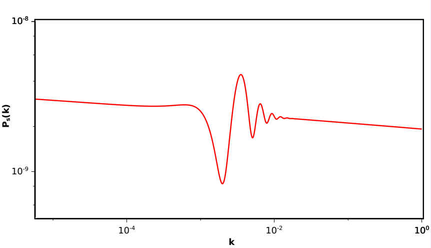

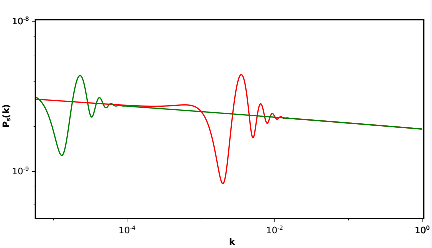

Effects of $\Delta\phi$

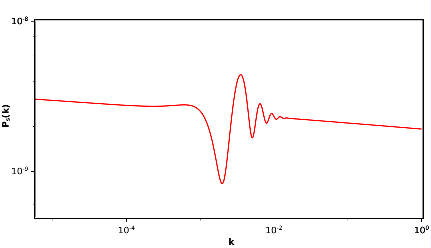

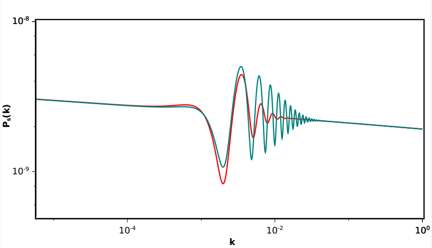

Which of these oscillations are favored by the CMB data?

- In the case of quadratic potential, it is known that introduction of the step improves the fit to the outliers near $\ell = 22$ and 40
- For example, it is found that χ^2_{eff} reduces by 7-8 when compared with a featureless, power law scalar spectrum

Aims of the work

The aims of our work are twofold:

- Firstly, we wish to examine whether, with the introduction of a step, other inflationary models too perform equally well against the CMB data, as the quadratic potential does.
- Secondly, the quadratic potential leads to a reasonable amount of tensors, and such a model will be ruled out if tensors are not detected corresponding to a tensor-to-scalar ratio of, say, $r \simeq 0.1$. So, we would also like to consider models that leads to a tensor-to-scalar ratio of $r < 0.1$, so that suitable alternative models exist if the tensors turn out to be small.

- We have evaluated the tensor contribution exactly for all the models, and have included it in our analysis

The inflationary models we have considered

- 1. Canonical scalars: Here we have considered the quadratic model
    $V(\phi) = (m^2\, \phi^2/2)$
    and the small field model
    $V(\phi) = V_0\, [1 - (\phi/\mu)^p]$
  2. Tachyon models[2]: In this case, the potentials we have considered are
    $V(\phi) = \left(\frac{\lambda}{\cosh\,(\phi/\phi_*)}\right)$
    and
    $V(\phi) = \left(\frac{\lambda}{1+(\phi/\phi_*)^4}\right)$
- All of them lead to slow roll
- We have introduced the step in each of these models and have compared them with the data.

[2] Steer et. al.(2004)

The tensor contribution

- As we mentioned, the quadratic model leads to a tensor-to-scalar ratio $r \simeq 0.1$
- The tachyon models too lead to a tensor-to-scalar ratio of $r \simeq 0.1$
- As we had pointed out, such models will be ruled out, if the tensors remain undetected at a level corresponding to a tensor-to-scalar ratio of, say, $r \simeq 0.1$
- Keeping this in mind, we have studied a small field model in our analysis where by choosing a specific μ and p we have restricted ourselves to a lower tensor-to-scalar ratio of $r \simeq 0.01$

The tensor amplitude in small field models[1]

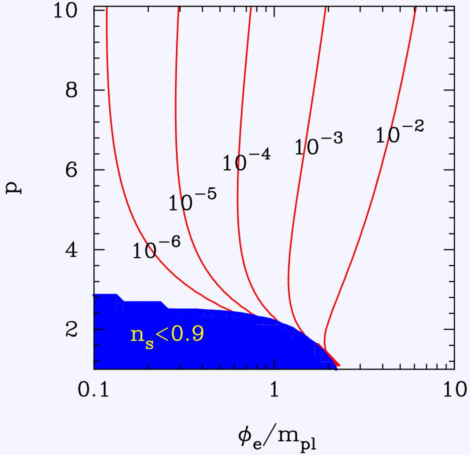

[1] Efstathiou et. al.(2006)

Methodology and datasets

- For our analysis, we have made use of the following datasets:
  1. WMAP-5
  2. WMAP-5 + QUaD-2009
  3. WMAP-5 + QUaD-2009 + ACBAR-2008
  4. WMAP-7
- We have calculated the scalar and tensor power spectra for all the models numerically with high accuracy.
- We have used publicly available CAMB and CosmoMC to compare our models with the data.
- We should mention that we have taken gravitational lensing and the SZ effect into account.

One dimensional likelihoods for the background parameters

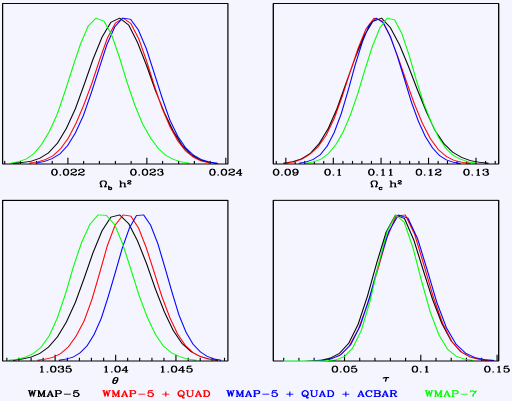

The one dimensional likelihood for the background parameters for the case of the small field model with the step.

One dimensional likelihood for α, ϕ_0 and $\Delta\phi$

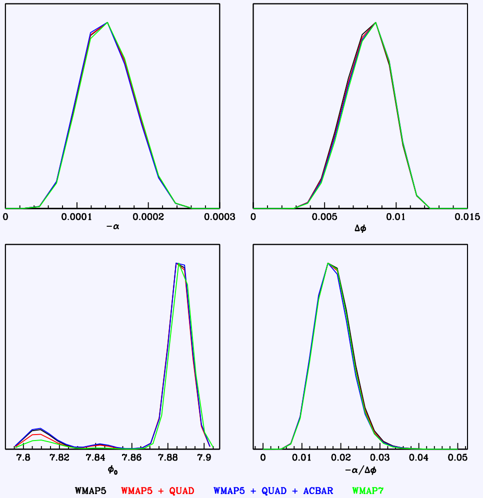

The χ^2_{eff} for the different models and datasets

Datasets / Models	WMAP-5	WMAP-5 + QUaD	WMAP-5 + QUaD + ACBAR	WMAP-7
PL $(4, 4)$	2658.40	2757.34	2779.12	7474.48
QP $(1, 1)$	2658.22 (-0.18)	2757.54 $(+0.20)$	2779.02 (-0.10)	7474.78 $(+0.30)$
QP + step $(4, 4)$	2651.00 (-7.40)	2750.38 (-6.96)	2771.72 (-7.40)	7466.28 (-8.20)
SFM $(3, 1)$	2658.26 (-0.14)	2757.46 $(+0.12)$	2779.06 (-0.06)	7474.78 $(+0.30)$
SFM + step $(6, 4)$	2650.96 (-7.44)	2750.26 (-7.08)	2771.92 (-7.20)	7466.00 (-8.48)
TM $(2, 1)$	2658.26 (-0.14)	2757.60 $(+0.26)$	2779.10 (-0.02)	7474.56 $(+0.08)$
TM + step $(5, 4)$	2651.14 (-7.26)	2750.50 (-6.84)	2772.06 (-7.06)	7465.92 (-8.56)

With the introduction of the step, χ^2_{eff} improves by 7-9 in all the cases. Note that the improvement is better for the WMAP-7 data than the WMAP-5 data.

Best fit primordial power spectra for all the models

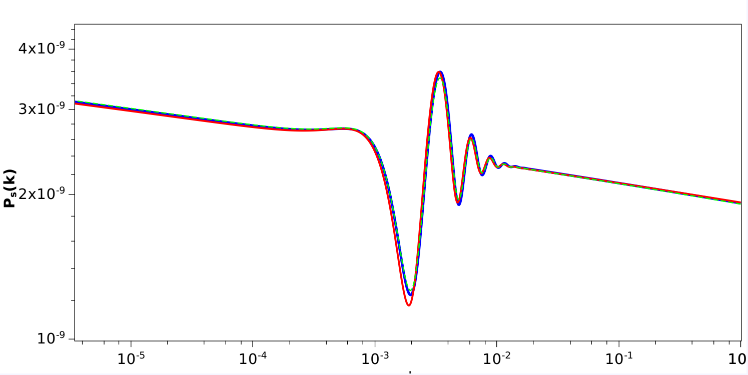

Quadratic model+step   Small field model+step   Tachyon model+step

The C_ℓ^{TT} for the best fit featureless power spectrum

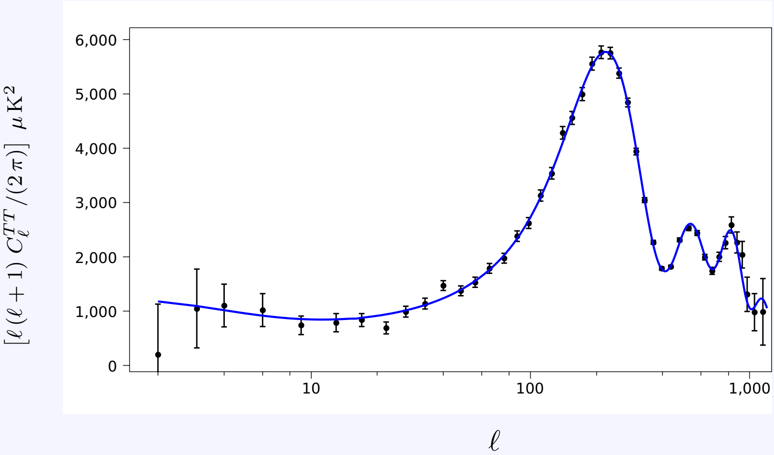

The quadratic model without step

The C_ℓ^{TT} for the best fit power spectrum with features

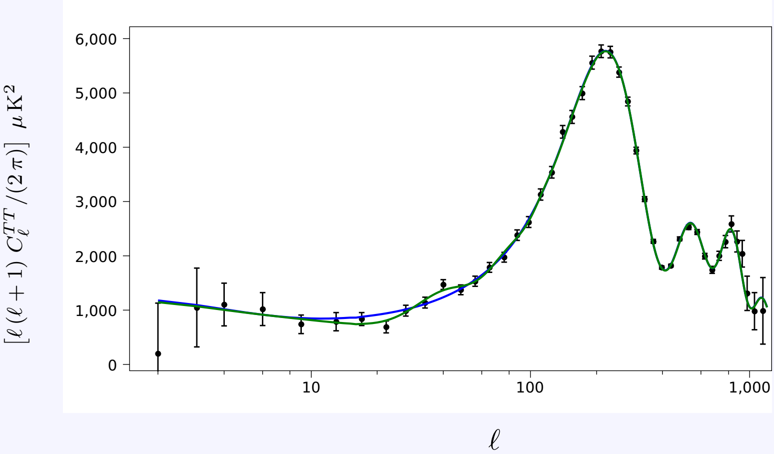

The quadratic model with step

The C_ℓ^{TT} for the best fit power spectrum with features

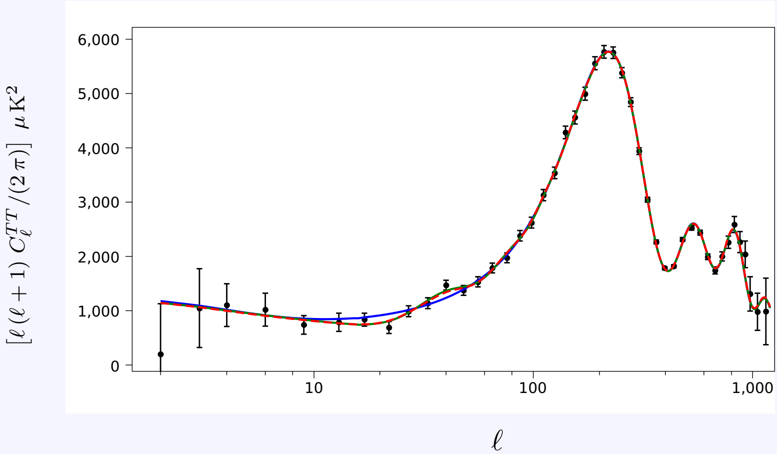

The quadratic model without step, quadratic model + step, small field model + step

Improvement in fit as a function of ℓ (WMAP-7)

- With the introduction of the step, we find that that most of the improvement in $\chi^2_{\rm eff}$ (by about 5-7) occurs over $\ell < 32$.
- For $\ell > 32$, the χ^2_{eff} improvement changes with ℓ as follows for the quadratic and the small field models.

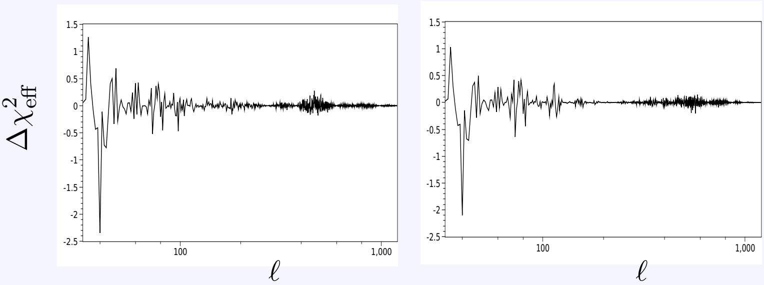

Summary and discussion

- Along with the quadratic model we have studied the effect of the step in a small field model and a tachyon model
- The step introduces a burst of oscillations and thus leaves its imprints on the CMB angular power spectrum
- Most of the improvement of fit come from the $\ell < 32$ and the rest comes from $\ell = 40$ (from the C_ℓ^{TT} spectrum only)
- Comparison with other datasets indicate that introduction of the step doesn't improve fits at higher ℓ 's (at least not as good as low ℓ)
- If ongoing (PLANCK) and/or future observations indicate that the amplitude of the tensor perturbations are rather small, then the quadratic potential and the tachyonic potentials will be ruled out, while a suitable small field model with a step will perform well against the data.
- Detection of large non-gaussianities will also put a restriction on the kind of inflation

1. Localized oscillations in the primordial power spectrum with a step
   - Slow-roll inflation
   - How features in the PPS can fit the outliers
   - Effects of the step
   - The goal of our project
   - Results
   - Summary and discussion
2. Non-local features
   - Possibilities of non-local features
   - Does the data support non-local features?
   - The goal of our project
   - Results
   - Summary and discussion
3. Calculating non-Gaussianities
   - Essentials
   - Calculating non-Gaussianities for the Starobinsky model
   - Our Numerical analysis
   - Summary and discussion

Based on work with M. Aich, L. Sriramkumar and T. Souradeep
Ref: arXiv:1106.2798v1 [astro-ph.CO]

Scope of this work: Can the spectrum contain non-local features?

- Apart from localized features, it is interesting to examine whether the CMB data also point to non-local features—i.e. certain characteristic and repeated behavior that extend over a wide range of scales—in the primordial spectrum

Scope of this work: Can the spectrum contain non-local features?

- Apart from localized features, it is interesting to examine whether the CMB data also point to non-local features—i.e. certain characteristic and repeated behavior that extend over a wide range of scales—in the primordial spectrum
- A quick glance at the unbinned CMB data seems to suggest that, after all, such an eventuality need not altogether be surprising.

Angular power spectrum from the WMAP 7-year data

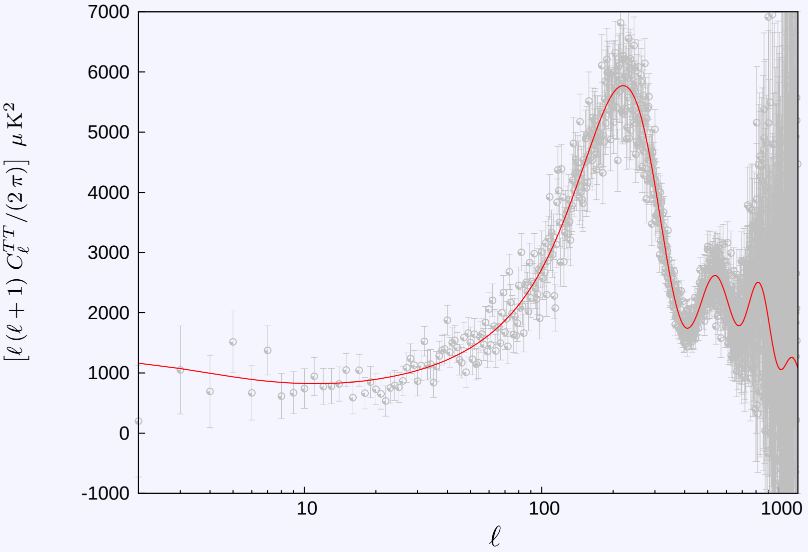

Scope of this work: Can the spectrum contain non-local features?

- Apart from localized features, it is interesting to examine whether the CMB data also point to non-local features—i.e. certain characteristic and repeated behavior that extend over a wide range of scales—in the primordial spectrum
- A quick glance at the unbinned CMB data seems to suggest that, after all, such an eventuality need not altogether be surprising.
- As the features we have considered in this work extends over all the scales it is important to have small scale CMB data to compare these features

WMAP-7 year data + ACT data

Constraint on Tensors

- Till now the tensor contribution from inflation is undetermined
- The tensor to scalar ratio $r < 0.3$ from WMAP-7
- Atacama Cosmology Telescope (ACT) probes as small scales data as $\ell \sim 10000$
- The joint constraint on r from WMAP-7 and ACT is < 0.24

Indication

As all the upper-bound quoted are at 95% CL Models with lower tensor contributions are becoming important to study

Does the data support non-local features?

Examples of certain non-local features

1. Superimposed Oscillations in the WMAP Data?[3]
2. Chaotic model with sinusoidal modulation[4]

Potential

$$V(\phi) = \frac{1}{2}\, m^2\, \phi^2 \left[1 + \alpha \, \sin\left(\frac{\phi}{\beta} + \delta\right)\right]$$

3. The axion monodromy model[5]

Potential

$$V(\phi) = \mu^3\phi + \Lambda^4 \cos\left(\frac{\phi}{\gamma} + \delta\right) = \lambda \left[\phi + \alpha \cos\left(\frac{\phi}{\beta} + \delta\right)\right]$$

[3] Martin et. al. 2003
[4] Pahud et. al. 2008
[5] Flauger et. al. 2009

Non-local features: The slow roll parameters

- The following two parameters characterize slow roll inflation

Hubble slow roll parameters

$$\epsilon = -\dot{H}/H^2, \qquad \eta = -\ddot{\phi}/H\dot{\phi}$$

If the inflaton is rolling slowly down a potential, then $(\epsilon,\ \eta) << 1$

- These models have oscillations in the potential and so the slow roll parameters are also oscillatory

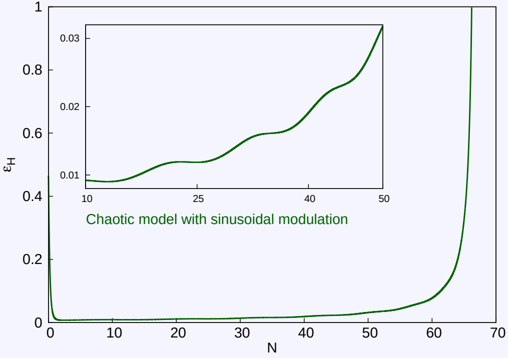

Which in turn leaves oscillations in the primordial power spectra

Non-local features: The slow roll parameters

- The following two parameters characterize slow roll inflation

Hubble slow roll parameters

$$\epsilon = -\dot{H}/H^2, \qquad \eta = -\ddot{\phi}/H\dot{\phi}$$

If the inflaton is rolling slowly down a potential, then $(\epsilon,\ \eta) << 1$

- These models have oscillations in the potential and so the slow roll parameters are also oscillatory

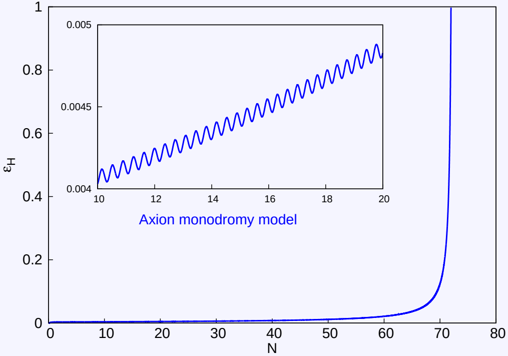

Which in turn leaves oscillations in the primordial power spectra

The spectral tilt, tensor to scalar ratio

- The spectral tilt in the case of the chaotic model with sine modulation comes out to be $n_s \simeq 0.96$
- Axion monodromy model produces a spectral tilt of $n_s \simeq 0.97$
- The tensor to scalar ratio (r) in the sine potential is $\simeq 0.16$ over the scales of cosmological interest
- Monodromy model produce $r \simeq 0.05 - 0.07$ over the same scales
- This model may perform better if the future CMB observations like PLANCK do not see a high tensor to scalar ratio
- We have evaluated the tensor modes for the two models exactly and used them to produce the angular power spectrum and included in our analysis

Aims of the work

The aims of our work are threefold:

Aims

1. We want to see how each model perform against the CMB datasets both at large and small scales. If the models perform better than the standard power law primordial spectrum we want to examine where from the improvements come
2. We have taken the tensor power spectrum into account to have a more realistic comparison
3. If the oscillations do give a better fit to the data than the standard case we would like to see if the oscillations can be constrained using the present datasets
   If not, then to forecast if the future datasets can, we have produced and used PLANCK mock data and have tested the models with the data

Methodology and datasets

- For our analysis, we have made use of the following datasets:
  1. WMAP-7
  2. WMAP-7 + Atacama Cosmology Telescope 148 GHz spectrum
- As the resulting PPS may contain violent oscillations depending on the frequency parameter β in the potential we must compute the PPS accurately
- We have calculated the scalar and tensor power spectra for all the models numerically with high accuracy
- We have used publicly available CAMB and CosmoMC to compare our models with the data
- We should mention that we have taken gravitational lensing and the SZ effect into account.

Results: The χ^2_{eff} for the different models and datasets

Datasets	WMAP-7	WMAP-7 + ACT
Power law case	7468.3	7500.4
Chaotic model with sine	7467.6 $(\Delta\chi^2_{eff} = 0.7)$	7498.2 $(\Delta\chi^2_{eff} = 2.2)$
Axion monodromy model	7462.1 $(\Delta\chi^2_{eff} = 6.2)$	7495.2 $(\Delta\chi^2_{eff} = 5.2)$

The chaotic model with the sinusoidal modulation provides a better fit of 0.7 over power law case

But the monodromy model provides a better fit of $\simeq 6$ over the same. So the oscillations here indeed provide a reasonable better fit to the data

Best fit primordial power spectra for all the models

The sine model, the axion monodromy model

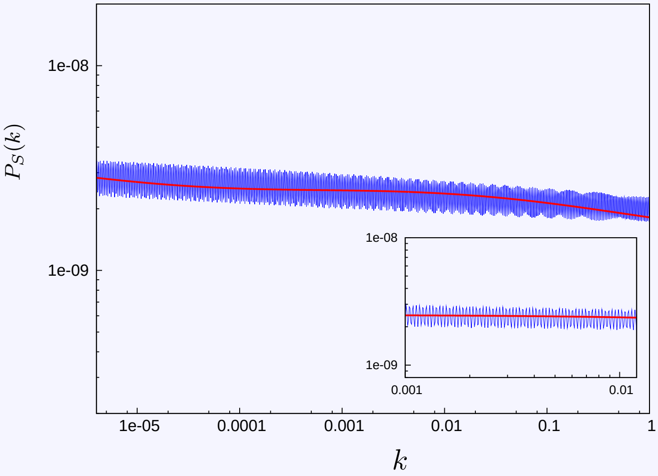

The C_ℓ^{TT} for the best fit models

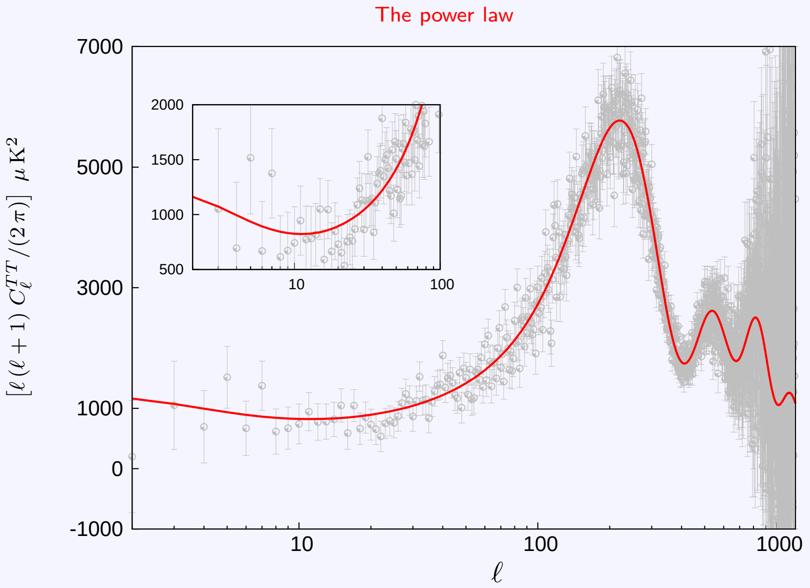

The C_ℓ^{TT} for the best fit models

The power law, the chaotic model with sine modulation

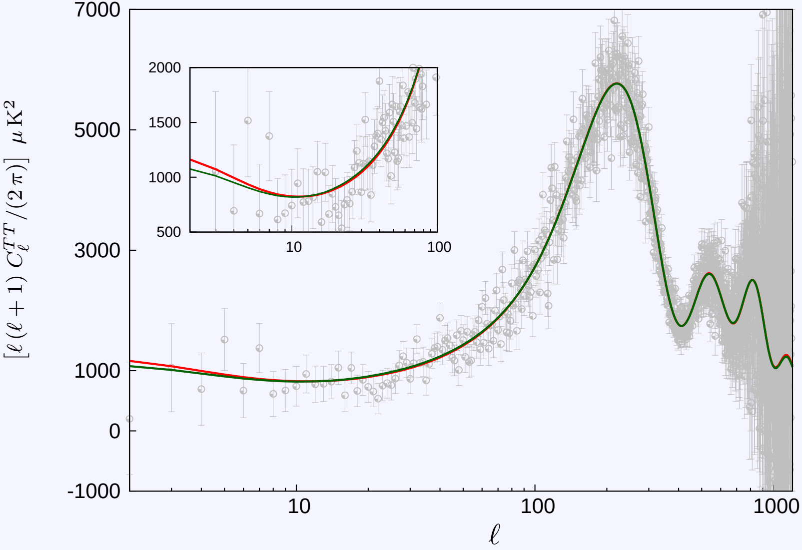

The C_ℓ^{TT} for the best fit models

The power law, the chaotic model with sine modulation, the axion monodromy model

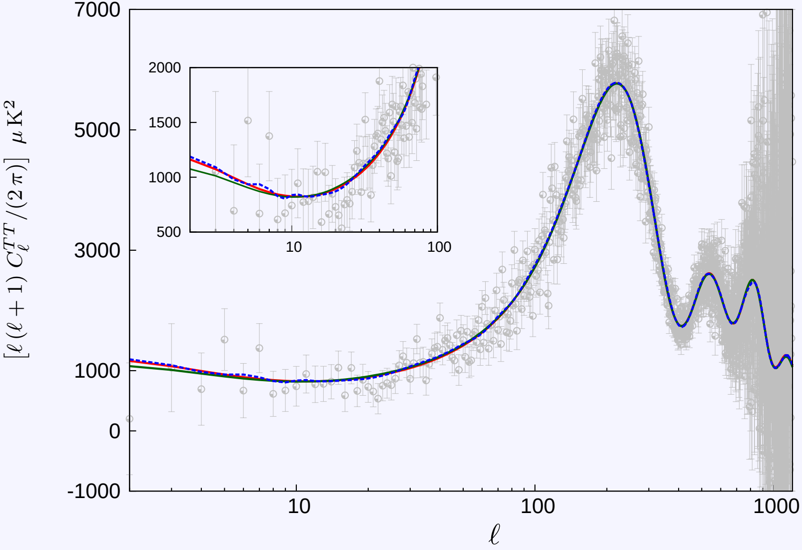

The $C_\ell^{TE/EE}$ best fit curves: The difference

The power law, the chaotic model with sine modulation, the axion monodromy model

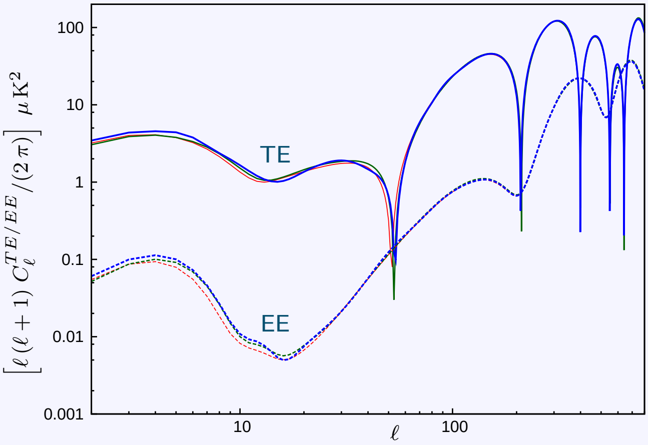

Improvement in fit as a function of ℓ (WMAP-7): TT

Sine model	Monodromy model
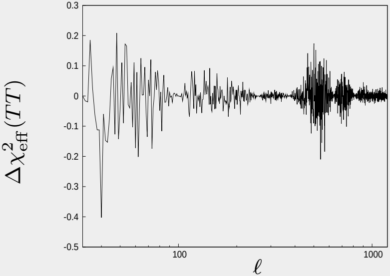	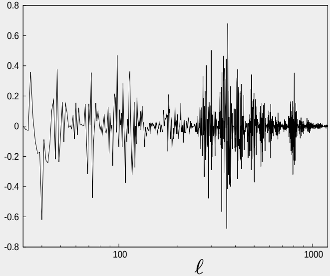

- The difference in the likelihood ($\Delta\chi^2_{\rm eff}(TT)$) for the sine model is not much both in the low as well as high ℓ's
- For the monodromy model,
  In the low ℓ ($\ell < 32$) the $\Delta\chi^2_{\rm eff}(TT) \simeq 3$
  In the high ℓ ($\ell > 32$) the $\Delta\chi^2_{\rm eff}(TT) \simeq 3$

Improvement in fit as a function of ℓ (WMAP-7): TE

Sine model	Monodromy model
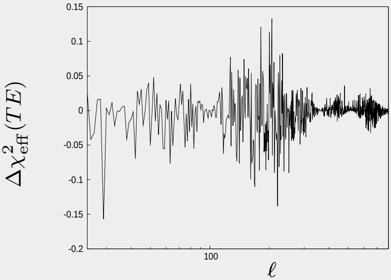	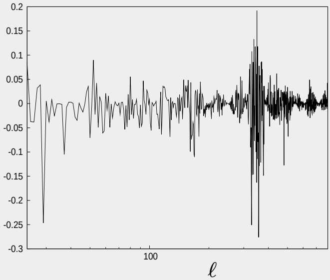

- For the sine model we get an overall improvement $\Delta\chi^2_{\rm eff}(TE) \simeq 1$
- In the case of monodromy model the improvement at high ℓ ($\ell > 24$) is nearly 3 But if we consider the low ℓ ($\ell < 24$) then there is no overall improvement from the TE spectrum

Forecast for PLANCK

- It is expected that data from current missions such as Planck would be able to constrain the cosmological parameters better
- We have used FuturCMB[1] add on with the CosmoMC to arrive at constraints on parameters
- The CMB angular power spectrum generated from the best fit parameters of the models using the WMAP seven year data is treated as the fiducial power spectrum for generating the PLANCK mock data

[1] Perotto et. al. (2006)

One dimensional likelihood

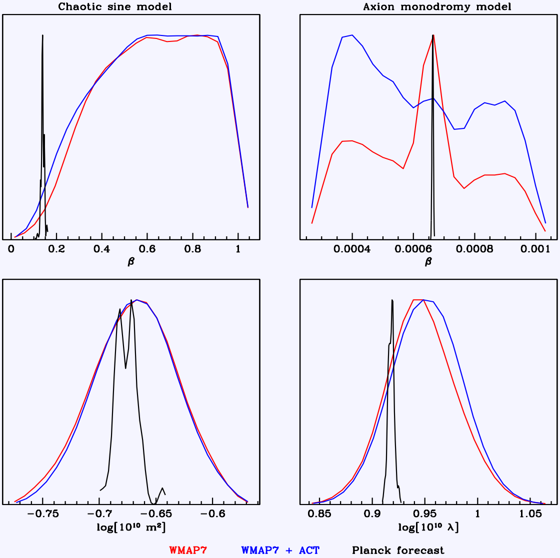

Two dimensional contours

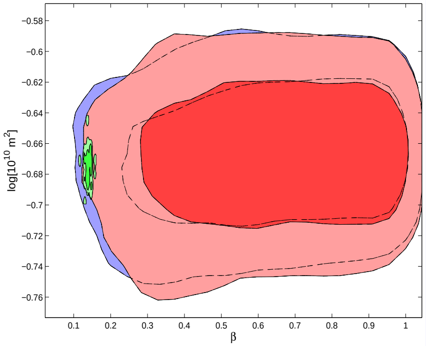

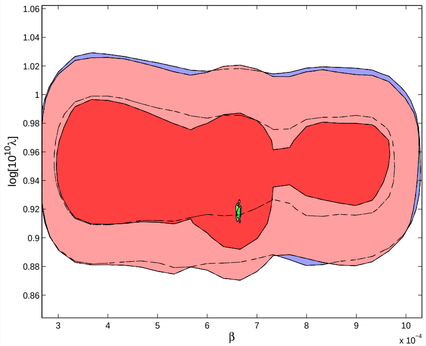

Sine model

Axion monodromy model

Constrains from WMAP-7, WMAP-7+ ACT, PLANCK mock data

Summary

- In this work we have studied the effect of the oscillations in the inflaton potential which creates oscillations in the primordial power spectrum and thereby produces oscillations in the CMB angular power spectrum
- These oscillations fit the CMB data better than the power law primordial power spectrum
- The better fit comes from both the low ℓ and the high ℓ s
- The $\Delta\chi^2_{\rm eff}(TT)$ suggests that the monodromy model is in better agreement with the data
- The improvement from the Atacama Cosmology Telescope data tells us that the sine model is more favored in the small scales than the monodromy model
- While the current data is not able to constrain the frequency of the models well enough, our result suggests with the future PLANCK data it will be possible to constrain the frequency
- If PLANCK is unable to see a high tensor to scalar ratio $r < 0.1$, the sine model will be discarded while the monodromy model will perform better than the conventional models

1 Localized oscillations in the primordial power spectrum with a step
- Slow-roll inflation
- How features in the PPS can fit the outliers
- Effects of the step
- The goal of our project
- Results
- Summary and discussion

2 Non-local features
- Possibilities of non-local features
- Does the data support non-local features?
- The goal of our project
- Results
- Summary and discussion

3 Calculating non-Gaussianities
- Essentials
- Calculating non-Gaussianities for the Starobinsky model
- Our Numerical analysis
- Summary and discussion

Work with L. Sriramkumar and J. Martin

Manuscript in preparation

Non-Gaussianities: Motivation

- The WMAP seven year data constrains the parameter $f_{\rm NL}$ that is often introduced to characterize the extent of non-Gaussianity in the primordial scalar power spectrum to be $f_{\rm NL} = (26 \pm 140)$ in the equilateral limit, at 68% confidence level
- It is often said that a large amount of non-Gaussianity, as possibly implied by the above mean value, will rule out inflationary models involving the canonical scalar field.
- Of course with the data form PLANCK we shall have a much better constraint on the parameter $f_{\rm NL}$
- It is known that single field inflationary models that lead to features in the scalar power spectrum (due to departures from slow roll) can produce large levels of non-Gaussianity

Non-Gaussianity: Essentials

- The scalar power spectrum $\mathcal{P}_{\rm S}(k)$ and the bi-spectrum $\mathcal{B}_{\rm S}(\mathbf{k}_1, \mathbf{k}_2, \mathbf{k}_3)$ are defined in terms of the two and three point correlation functions of the Fourier modes of the curvature perturbation $\mathcal{R}$ as follows

Three point correlation functions

$$\begin{aligned}
\langle \hat{\mathcal{R}}_{\mathbf{k}}\, \hat{\mathcal{R}}_{\mathbf{p}} \rangle &= \frac{(2\,\pi)^2}{2\,k^3}\, \mathcal{P}_{\rm S}(k)\; \delta^{(3)}\left(\mathbf{k}+\mathbf{p}\right),\\
\langle \hat{\mathcal{R}}_{\mathbf{k}_1}\, \hat{\mathcal{R}}_{\mathbf{k}_2}\, \hat{\mathcal{R}}_{\mathbf{k}_3} \rangle &= (2\,\pi)^3\;\, \mathcal{B}_{\rm S}(\mathbf{k}_1, \mathbf{k}_2, \mathbf{k}_3)\\
&\qquad \times \delta^{(3)}\left(\mathbf{k}_1+\mathbf{k}_2+\mathbf{k}_3\right),
\end{aligned}$$

where $k = |\mathbf{k}|$. The non-Gaussianity parameter $f_{_{\rm NL}}$ is introduced through the relation

The $f_{_{\rm NL}}$

$$\mathcal{R} = \mathcal{R}^{\rm G} - \frac{3\, f_{_{\rm NL}}}{5}\, \left[\mathcal{R}^{\rm G}\right]^2$$

Non-Gaussianity: Essentials

Upon using this relation, and the definitions of the power spectrum and the bi-spectrum above, one can arrive at the expression for the parameter $f_{_{\rm NL}}$ in terms of the power spectrum and the bi-spectrum

In the equilateral limit , i.e. when $\mathbf{k}_1 = \mathbf{k}_2 = \mathbf{k}_3 = \mathbf{k}$, it is found to be

Expression of $f_{_{\rm NL}}$

$$f_{_{\rm NL}} = -\left(\frac{10}{9}\right)\,\left(\frac{1}{(2\,\pi)^4}\right)\,\left(\frac{k^6\,G(k)}{\mathcal{P}_{_{\rm S}}^2(k)}\right),$$

where $G(k) = [(2\,\pi)^{9/2}\,\mathcal{B}_{_{\rm S}}(k)]$.

Calculating non-Gaussianity: The standard procedure

There now exists a standard procedure for evaluating the scalar bi-spectrum in inflationary models[1]

The quantity $G(k)$, evaluated towards the end of inflation at the conformal time, say, $\eta = \eta_{\rm e}$, can be written as

Definition of $G(k)$

$$
\begin{aligned}
G(k) &\equiv \sum_{C=1}^{6} G_{_C}(k) \\
&= M_{_{\rm Pl}}^{2} \sum_{C=1}^{6} \left[f_k^{3}(\eta_{\rm e})\, \mathcal{G}_{_C}(k) + f_k^{*3}(\eta_{\rm e})\, \mathcal{G}_{_C}^{*}(k)\right]
\end{aligned}
$$

[1] Maldacena (2003)

The action at the cubic order[1]

It can be shown that the third order term in the action describing the curvature perturbations is given by

$$\mathcal{S}_3[\mathcal{R}] = M_{_{\rm Pl}}^2 \int {\rm d}\eta \int {\rm d}^3\mathbf{x} \biggl[a^2\, \epsilon_1^2\, \mathcal{R}\, \mathcal{R}'^2 + a^2\, \epsilon_1^2\, \mathcal{R}\, (\partial\mathcal{R})^2 - 2\, a\, \epsilon_1\, \mathcal{R}'\, (\partial^i\mathcal{R})\, (\partial_i\chi)$$
$$+ \frac{a^2}{2}\, \epsilon_1\, \epsilon_2'\, \mathcal{R}^2\, \mathcal{R}' + \frac{\epsilon_1}{2}\, (\partial^i\mathcal{R})\, (\partial_i\chi)\, (\partial^2\chi) + \frac{\epsilon_1}{4}\, (\partial^2\mathcal{R})\, (\partial\chi)^2 + \mathcal{F}\left(\frac{\delta\mathcal{L}_2}{\delta\mathcal{R}}\right)\biggr]$$

where $\mathcal{F}(\delta\mathcal{L}_2/\delta\mathcal{R})$ denotes terms involving the variation of the second order action with respect to $\mathcal{R}$, while χ is related to the curvature perturbation $\mathcal{R}$ through the relations

$$\Lambda = a\, \epsilon_1\, \mathcal{R}' \quad \text{and} \quad \partial^2\chi = \Lambda.$$

[1] Maldacena(2003); Seery et. al. (2005); Chen et.al. (2007)

All contributions

$$
\begin{aligned}
\mathcal{G}_1(\mathbf{k}) &= 2i\int_{\eta_{\rm in}}^{\eta_{\rm e}} \mathrm{d}\tau\, a^2\, \epsilon_1^2\, \left(f_{k_1}^*\, f_{k_2}'^*\, f_{k_3}'^* + \text{two perm}\right)\\
\mathcal{G}_2(\mathbf{k}) &= -2i\int_{\eta_{\rm in}}^{\eta_{\rm e}} \mathrm{d}\tau a^2\, \epsilon_1^2\, f_{k_1}^*\, f_{k_2}^*\, f_{k_3}^*\, \left(\mathbf{k}_1\cdot\mathbf{k}_2 + \text{two perm}\right)\\
\mathcal{G}_3(\mathbf{k}) &= -2i\int_{\eta_{\rm in}}^{\eta_{\rm e}} \mathrm{d}\tau\; a^2\, \epsilon_1^2\, \left[f_{k_1}^*\, f_{k_2}'^*\, f_{k_3}'^*\, \left(\frac{\mathbf{k}_1\cdot\mathbf{k}_2}{k_2^2}\right) + \text{five perm}\right]\\
\mathcal{G}_4(\mathbf{k}) &= i\int_{\eta_{\rm in}}^{\eta_{\rm e}} \mathrm{d}\tau\; a^2\, \epsilon_1\, \epsilon_2'\, \left(f_{k_1}^*\, f_{k_2}^*\, f_{k_3}'^* + \text{two perm}\right)\\
\mathcal{G}_5(\mathbf{k}) &= \frac{i}{2}\int_{\eta_{\rm in}}^{\eta_{\rm e}} \mathrm{d}\tau\; a^2\, \epsilon_1^3\, \left[f_{k_1}^*\, f_{k_2}'^*\, f_{k_3}'^*\, \left(\frac{\mathbf{k}_1\cdot\mathbf{k}_2}{k_2^2}\right) + \text{five perm}\right]\\
\mathcal{G}_6(\mathbf{k}) &= \frac{i}{2}\int_{\eta_{\rm in}}^{\eta_{\rm e}} \mathrm{d}\tau\; a^2\, \epsilon_1^3\, \left[f_{k_1}^*\, f_{k_2}'^*\, f_{k_3}'^*\, \left(\frac{k_1^2}{k_2^2\, k_3^2}\right)\, (\mathbf{k}_2\cdot\mathbf{k}_3) + \text{two perm}\right]\\
G_7(\mathbf{k}) &= \frac{\epsilon_2}{2}\left(|f_{k_2}|^2\, |f_{k_3}|^2 + \text{two perm}\right)
\end{aligned}
$$

The Starobinsky model[1]

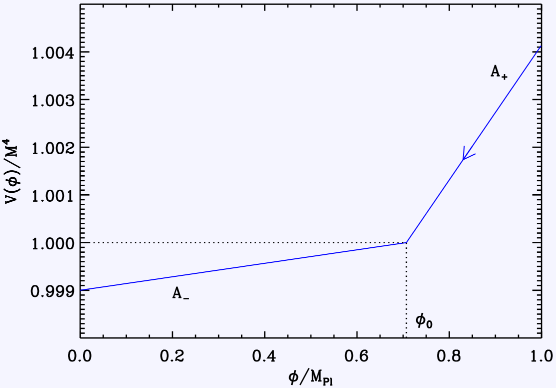

The Starobinsky model involves the canonical scalar field which is described by the potential

$$V(\phi) = \begin{cases} V_0 + A_+\,(\phi - \phi_0) & \text{for } \phi > \phi_0, \\ V_0 + A_-\,(\phi - \phi_0) & \text{for } \phi < \phi_0. \end{cases}$$

[1] Starobinsky(1992); Work of Martin and Sriramkumar (in preparation)

Assumptions and properties[1]

- It is assumed that the constant V_0 is the dominant term in the potential for a range of ϕ near ϕ_0. As a result, over the domain of our interest, the expansion is of the de Sitter form corresponding to a Hubble parameter H_0 determined by V_0.
- The scalar field rolls slowly until it reaches the discontinuity in the potential. It then fast rolls for a brief period as it crosses the discontinuity before slow roll is restored again.
- Since V_0 is dominant, the first slow roll parameter ϵ_1 remains small even during the transition. This property allows the background to be evaluated analytically to a good approximation.

[1] Work of Martin and Sriramkumar (in preparation)

Analytic expressions for the slow roll parameters

Under the assumptions and approximations described above, the slow roll parameters remain small before the transition.

Analytic expressions for the slow roll parameters

Under the assumptions and approximations described above, the slow roll parameters remain small before the transition.

One can show that, after the transition, the evolution of the first slow roll parameter ϵ_1 can be expressed in terms of the number of e-folds N as follows:

$$\epsilon_{1-} \simeq \frac{A_-^2}{18\, M_{\rm Pl}^2\, H_0^4}\, \left[1 - \frac{\Delta A}{A_-}\, {\rm e}^{-3\,(N-N_0)}\right]^2,$$

where $\Delta A = (A_- - A_+)$, while N_0 is the e-fold at which the field crosses the discontinuity.

Analytic expressions for the slow roll parameters

Under the assumptions and approximations described above, the slow roll parameters remain small before the transition.

One can show that, after the transition, the evolution of the first slow roll parameter ϵ_1 can be expressed in terms of the number of e-folds N as follows:

$$\epsilon_{1-} \simeq \frac{A_-^2}{18\, M_{\rm Pl}^2\, H_0^4}\, \left[1 - \frac{\Delta A}{A_-}\, {\rm e}^{-3\,(N-N_0)}\right]^2,$$

where $\Delta A = (A_- - A_+)$, while N_0 is the e-fold at which the field crosses the discontinuity.

It is found that, *immediately after the transition*, the second slow roll parameter ϵ_2 is given by

$$\epsilon_{2-} \simeq \frac{6\,\Delta A}{A_-}\, \frac{{\rm e}^{-3\,(N-N_0)}}{1 - (\Delta A/A_-)\, {\rm e}^{-3\,(N-N_0)}}.$$

Evolution of the slow roll parameters[1]

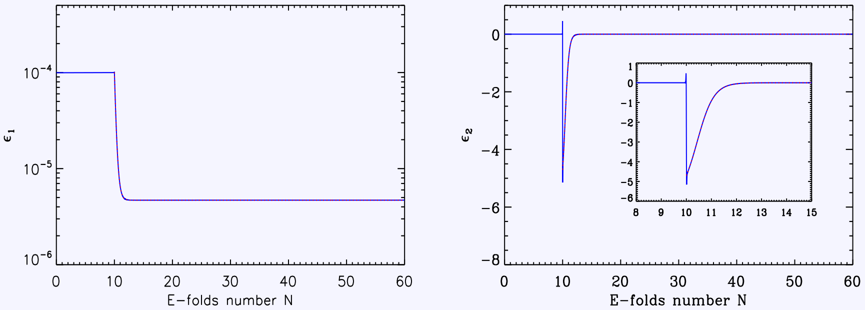

The evolution of the first slow roll parameter ϵ_1 on the left, and the second slow roll parameter ϵ_2 on the right in the Starobinsky model. While the blue curves describe the numerical results, the dotted red curves represent the analytical expressions mentioned in the previous slide.

[1] Work of Martin and Sriramkumar (in preparation)

The modes before and after the transition

It can be shown that, under the assumptions that one is working with, the quantity $z = a\, M_{_{\rm Pl}}\, \sqrt{2\, \epsilon_1}$, which determines the evolution of the perturbations, simplifies to

$$z''/z \simeq 2\, \mathcal{H}^2$$

both before *as well as* after the transition with the overprime denoting the derivative with respect to the conformal time, while $\mathcal{H}$ is the conformal Hubble parameter.

The modes before and after the transition

It can be shown that, under the assumptions that one is working with, the quantity $z = a\, M_{\rm Pl}\, \sqrt{2\, \epsilon_1}$, which determines the evolution of the perturbations, simplifies to

$$z''/z \simeq 2\, \mathcal{H}^2$$

both before *as well as* after the transition with the overprime denoting the derivative with respect to the conformal time, while $\mathcal{H}$ is the conformal Hubble parameter.

As a result, while the solution to the Mukhanov-Sasaki variable v_k before the transition is given by

$$v_k^{+}(\eta) = \frac{1}{\sqrt{2\, k}}\, \left(1 - \frac{i}{k\, \eta}\right)\, {\rm e}^{-i\, k\, \eta},$$

after the transition, it can be expressed as a linear combination of the positive and the negative frequency modes as follows:

$$v_k^{-}(\eta) = \frac{\alpha_k}{\sqrt{2\, k}}\, \left(1 - \frac{i}{k\, \eta}\right) {\rm e}^{-i\, k\, \eta} + \frac{\beta_k}{\sqrt{2\, k}}\, \left(1 + \frac{i}{k\, \eta}\right) {\rm e}^{i\, k\, \eta}$$

where α_k and β_k are the usual Bogoliubov coefficients.

The scalar power spectrum in the Starobinsky model

The Bogoliubov coefficients α_k and β_k can be obtained by matching the mode v_k and its derivative at the transition.

The scalar power spectrum in the Starobinsky model

The Bogoliubov coefficients α_k and β_k can be obtained by matching the mode v_k and its derivative at the transition.

The scalar power spectrum, given by

$$\mathcal{P}_{\rm S}(k) = (k^3/2\,\pi^2)\,|\mathcal{R}_k|^2 = (k^3/2\,\pi^2)\,(|v_k|/z)^2$$

where $\mathcal{R}_k$ is the curvature perturbation, can be evaluated at late times to be

$$\mathcal{P}_{\rm S}(k) = \left(\frac{9\,H_0^6}{4\,\pi^2\,A_-^2}\right)\,\left\{1 - \frac{3\,\Delta A}{A_+}\,\frac{k_0}{k}\left[\left(1-\frac{k_0^2}{k^2}\right)\,\sin\left(\frac{2\,k}{k_0}\right) + \frac{2\,k_0}{k}\cos\left(\frac{2\,k}{k_0}\right)\right]\right.$$
$$+\frac{9\,\Delta A^2}{2\,A_+^2}\,\frac{k_0^2}{k^2}\,\left(1+\frac{k_0^2}{k^2}\right)\,\left[\left(1+\frac{k_0^2}{k^2}\right) - \frac{2\,k_0}{k}\,\sin\left(\frac{2\,k}{k_0}\right)\right.$$
$$\left.\left. + \left(1-\frac{k_0^2}{k^2}\right)\,\cos\left(\frac{2\,k}{k_0}\right)\right]\right\}$$

where k_0 is the wavenumber of the mode that crosses the Hubble radius when the field crosses the discontinuity. Note that the power spectrum depends on the wavenumber only through the ratio (k/k_0).

Comparison with the numerical result[1]

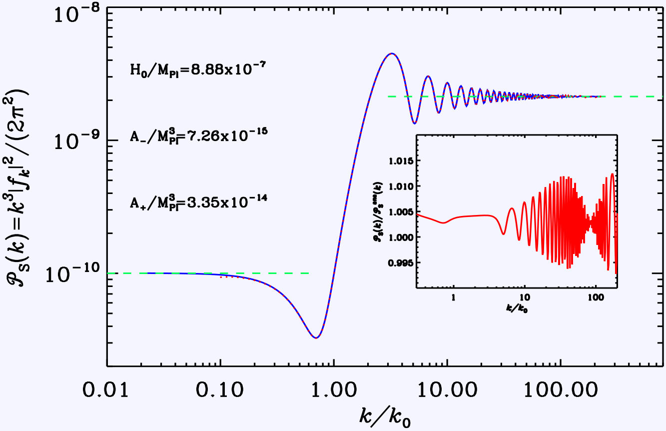

The scalar power spectrum in the Starobinsky model. While the blue solid curve denotes the analytic result, the red dots represent the corresponding numerical scalar power spectrum

[1] Work of Martin and Sriramkumar (in preparation)

The non-Gaussian terms for the Starobinsky model[1]

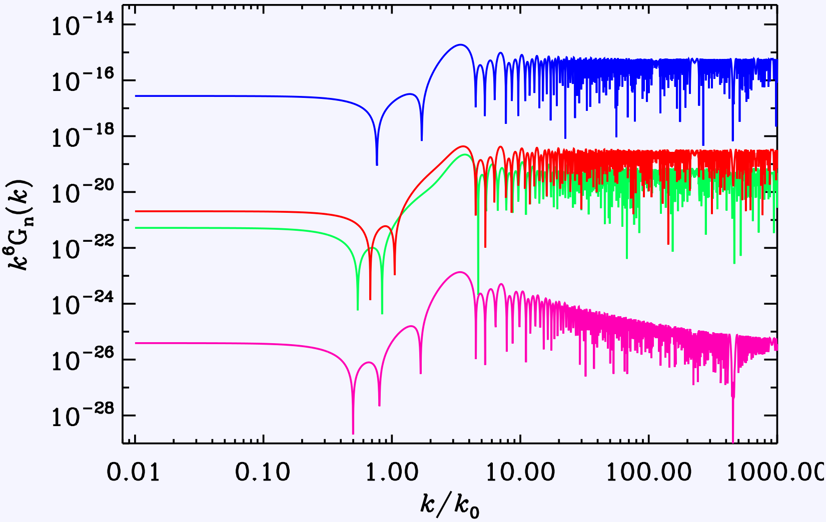

[1] Work of Martin and Sriramkumar (in preparation)

The $f_{\rm NL}$ for the Starobinsky model[1]

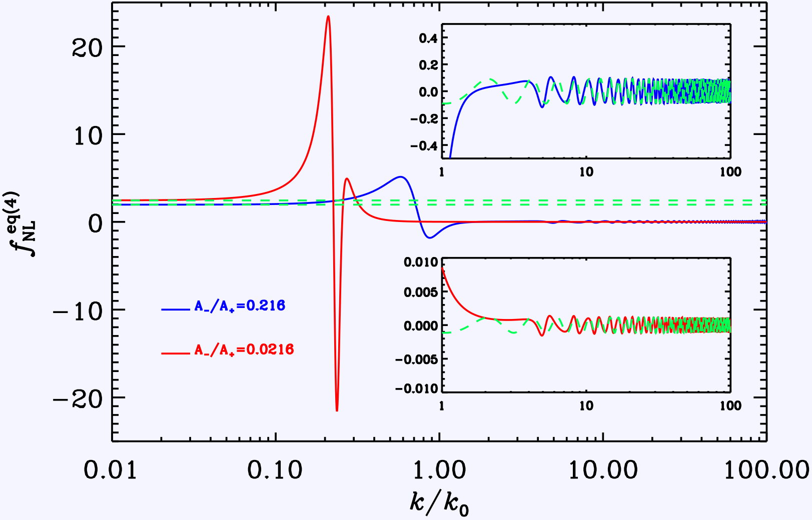

[1] Work of Martin and Sriramkumar (in preparation)

Numerical calculation of non-Gaussianities: Our work

1. With the PLANCK map it might be possible to detect the non-Gaussianities (specifically the $f_{\rm NL}$) $\mathcal{O}(1)$
2. The error bars are expected to shrink to ± 3
3. Now it is very important to develop a platform to calculate the $f_{\rm NL}$ with high accuracy
4. Our recent work has been based on the the complete numerical evaluation of non-Gaussianities for a general single canonical scalar field driven inflation
5. We have developed a very fast code which can calculate the all contributions of the three point correlation function for any single canonical scalar field inflation
6. This code does not assume any approximation such as slow roll etc. We have used the adaptive quadrature routine to calculate the three point function and we have used $e - folds$ as the parameter of integration.

Inflationary models leading to features[1]

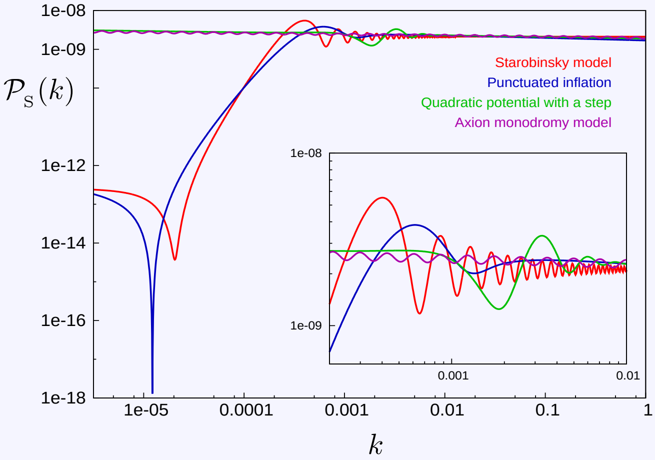

The scalar power spectra in a few different inflationary models that leads to better fit when compared to power law primordial spectrum.

[1] Jain et al. (2009); Hazra et al (2010); Aich et al. (2011)

Comparison with the analytical results: The Starobinsky model

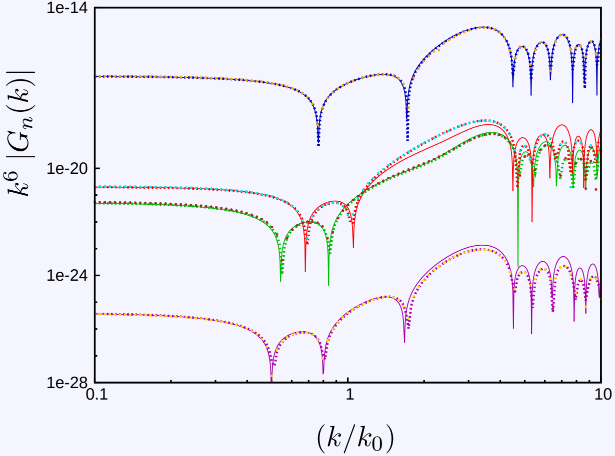

The quantities k^6 times the absolute values of $(G_1 + G_3)$ (in green), G_2 (in red), G_4 (in blue) and $(G_5 + G_6)$ (in purple) have been plotted as a function of (k/k_0) for the Starobinsky model. Note that k_0 is the wavenumber which leaves the Hubble radius when the scalar field crosses the break in the potential.

The non-Gaussian contributions for the punctuated Inflation model

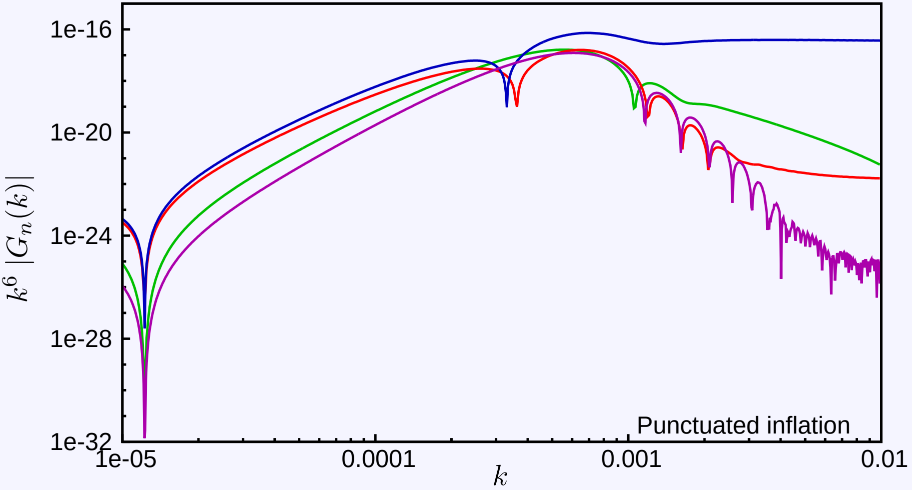

The non-Gaussian contributions for the quadratic potential with a step

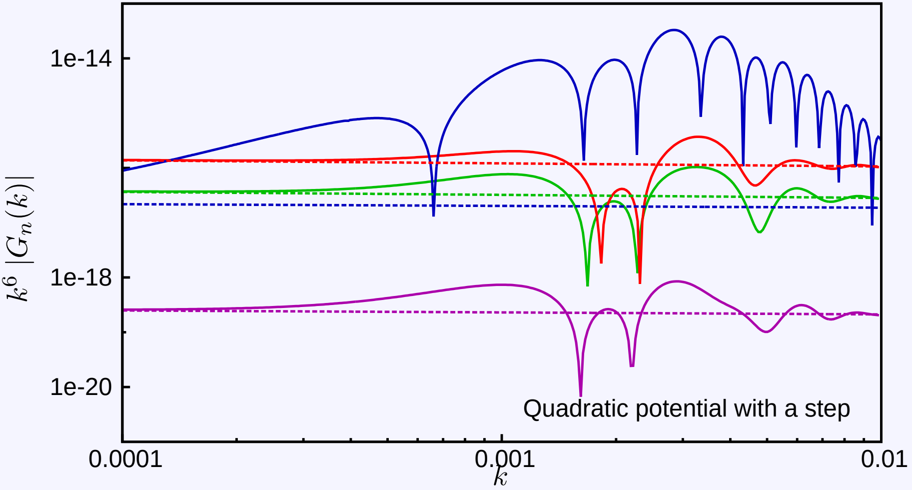

The non-Gaussian contributions for the axion monodromy model

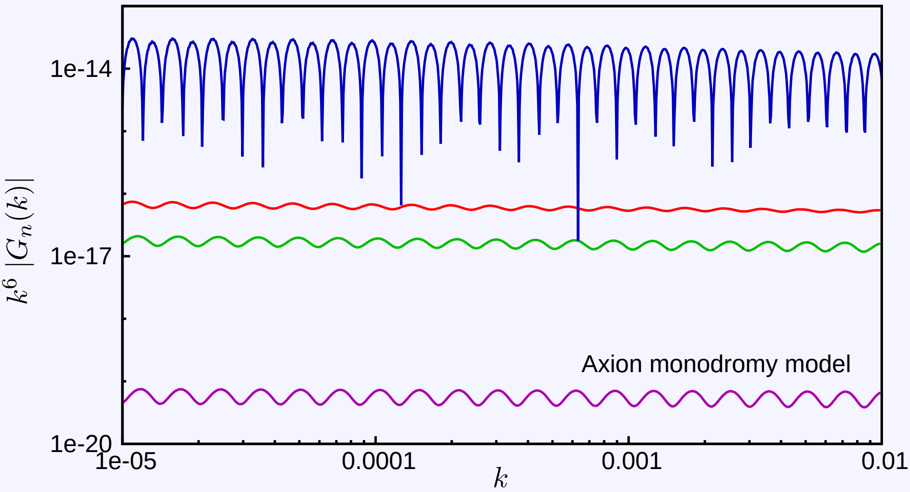

The $f_{\rm NL}$ for the punctuated inflation model

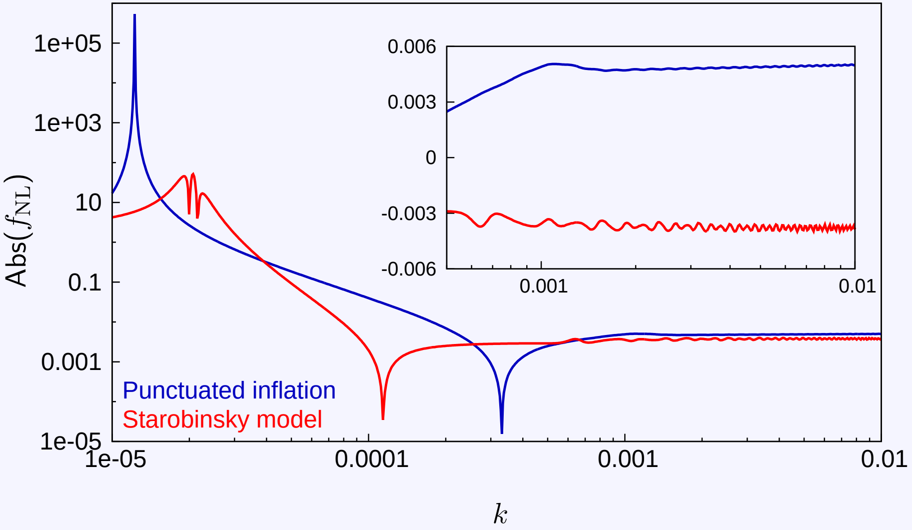

The f_{NL} for the models with step

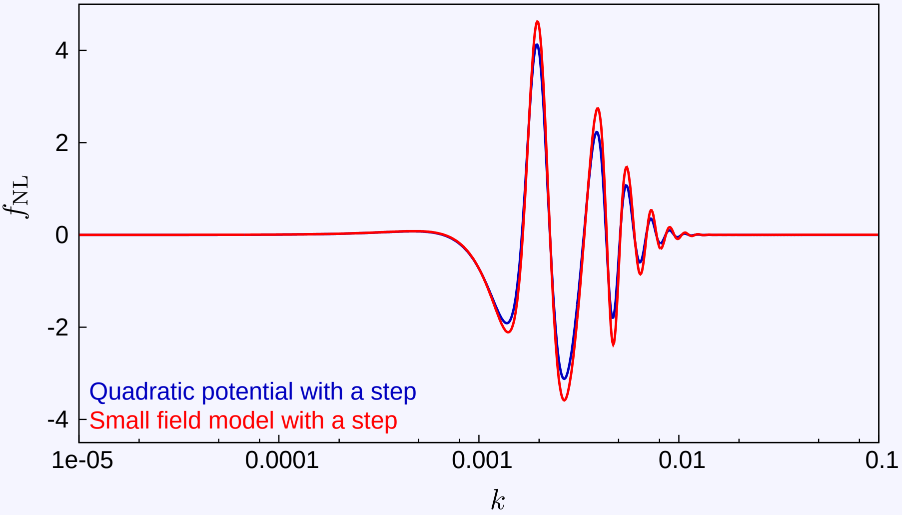

The $f_{\rm NL}$ for the axion monodromy model

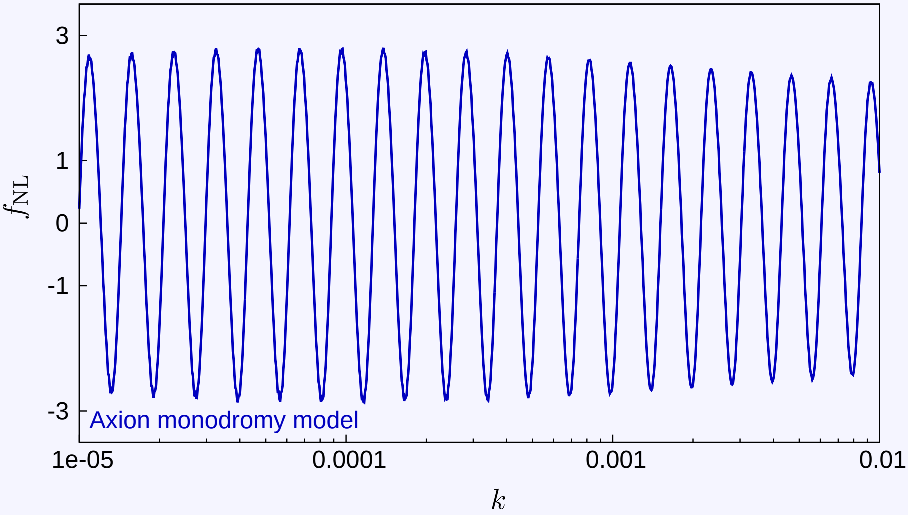

Summary and discussion

- We have produced a fast and accurate code to calculate the non-Gaussianities for every single canonical scalar field driven inflation in the equilateral limit
- Given a potential and the initial field value it can calculate all the non-Gaussian contribution that arise from the cubic order action
- We have extended the code and produced a distributed memory parallel program to calculate the $f_{\rm NL}$ for arbitrary configuration (*i.e.* squeezed, scalene etc.)
- As we are going to have much better data with the PLANCK results very soon, along with the angular power spectrum the $f_{\rm NL}$ can become an useful factor to constraining the list of inflationary models

Thank you for your attention